Clarke Circuit Analysis for Space-Vector Ellipse Characterization of Phase-to-Ground Faults in Three-Phase Radial Systems

DIEGO BELLAN
Department of Electronics, Information and Bioengineering,
Politecnico di Milano,
Piazza Leonardo da Vinci 32, 20133 Milan,
ITALY

Abstract: - This work deals with the technique for fault detection and classification in three-phase power systems based on the elliptical trajectory of the voltage space vector on the complex plane. A new approach is presented leading to the derivation of equivalent circuits directly in the Clarke domain where the space vector is defined. A specific methodology is introduced to manage the asymmetrical behavior of single-phase and double-phase faults. In particular, an in-depth analysis is presented for the single-phase-to-ground fault. The proposed equivalent circuits allow straightforward derivation and interpretation of the voltage ellipse for fault characterization. The analytical results are validated through the simulation of a three-phase radial system.

Key-Words: - Clarke transformation, fault analysis, power quality, power system analysis, space vectors, voltage sags.

Received: February 21, 2023. Revised: November 29, 2023. Accepted: December 15, 2023. Published: December 31, 2023.

1 Introduction

Power quality is a major issue in modern power systems. Extensive literature is available about disturbance analysis and classification techniques, [1], [2], [3], [4], [5], [6], [7], [8], [9], [10], [11], [12]. In recent years, one of the most interesting and promising methodologies for disturbance detection and classification is the approach based on the analysis of space vector trajectories on the complex plane, [13], [14], [15], [16], [17], [18], [19], [20], [21], [22], [23]. Although the space vector technique has been proposed for several kinds of disturbances, the straightforward application of such technique is in the detection and classification of voltage sags due to fault conditions. Indeed, the basic principle of the space vector methodology consists of the observation that, under fault conditions, the voltage space vector traces an elliptical trajectory on the complex plane. The inclination angle of such an ellipse allows the classification of the fault. Figure 1 shows the characteristic inclination angle of the space vector ellipse for different kinds of single-phase (Sa, Sb, Sc) and double-phase (Dab, Dbc, Dac) faults, [23].

In the relevant literature the relationship between the faulted three-phase system and the inclination of the voltage space-vector ellipse is obtained in two steps, [20], [22]. First, a simplified three-phase faulted circuit is solved through conventional techniques in the original abc domain of voltage/current variables. Second, the Clarke transformation is used to obtain analytical expressions for the voltage space-vector components on the complex plane. Such an approach leads to correct results, but since the circuits are solved in the original abc domain they cannot provide direct insight into the space vector components because the space vector is defined on the Clarke transformed variables α and β. In other terms, the conventional approach does not provide equivalent circuits in the Clarke transformed variables, thus the circuit interpretation of the space vector trajectory is prevented.

In this paper, a circuit methodology directly based on the Clarke transformed variables is proposed. In particular, the methodology is derived in detail for single-phase grounded faults. Equivalent circuits are derived directly in the Clarke variables $\alpha\beta 0$ domain. A specific approach is described to manage the asymmetrical behavior of a single-phase fault. The proposed approach allows the straightforward determination of the voltage alpha and beta components leading to the definition of the space vector. Thus, a direct link is established between equivalent circuits and space vector properties. Notice that this paper provides a methodological contribution, whereas analytical evaluations concerning the single-phase fault can be equivalently performed through the conventional approach proposed in [16].

The paper is organized as follows. In Section II the Clarke transformation and its conventional use in the analysis of symmetrical circuits is recalled. In Section III the use of the Clarke transformation is extended to the case of an asymmetrical component such as a single-phase fault. Specific equivalent circuits in the Clarke domain are derived to take into account such asymmetrical behavior. In Section IV the proposed methodology is used to analyze fault conditions in a simple radial system, and some properties of the space vector ellipses are put in relation with the derived equivalent circuits in the Clarke domain. Finally, discussion and concluding remarks are drawn in Section V.

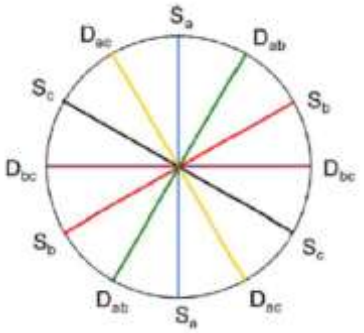

Fig. 1: Inclination angle of the voltage space-vector ellipse for different kinds of single-phase (S_a, S_b, S_c) and double-phase (D_{ab}, D_{bc}, D_{ac}) faults

2 Topological Properties of Clarke Transformed Three-Phase Circuits

Let us consider a column vector $\boldsymbol{v} = [v_a \quad v_b \quad v_c]^T$ of phase voltages across a three-phase component in the time domain. The Clarke transformation of $\boldsymbol{v}$ is defined as, [24]:

$$\boldsymbol{v}_T = \begin{bmatrix} v_\alpha \\ v_\beta \\ v_0 \end{bmatrix} = \sqrt{\frac{2}{3}} \begin{bmatrix} 1 & -\frac{1}{2} & -\frac{1}{2} \\ 0 & \frac{\sqrt{3}}{2} & -\frac{\sqrt{3}}{2} \\ \frac{1}{\sqrt{2}} & \frac{1}{\sqrt{2}} & \frac{1}{\sqrt{2}} \end{bmatrix} \begin{bmatrix} v_a \\ v_b \\ v_c \end{bmatrix} = \boldsymbol{T}\boldsymbol{v} \qquad (1)$$

Notice that the transformation matrix $\boldsymbol{T}$ is defined in its rational form, i.e., with the coefficient $\sqrt{2/3}$ which guarantees the orthogonality property $\boldsymbol{T}^{-1} = \boldsymbol{T}^T$. It can be readily shown that the orthogonality property results in conservation of power from the *abc* domain to the transformed $\alpha\beta 0$ domain. This is a crucial point in view of deriving coherent equivalent circuits in the $\alpha\beta 0$ domain.

When a basic and symmetrical three-phase component is considered, the Clarke transformation operates the diagonalization of the matrix component. For example, by considering an inductive symmetrical component (i.e., a component with equal self-inductances L_{ph}, and equal mutual inductances L_m), the Clarke transformation provides:

$$\boldsymbol{v}_T = \begin{bmatrix} v_\alpha \\ v_\beta \\ v_0 \end{bmatrix} = \boldsymbol{T}\boldsymbol{v} =$$

$$= \boldsymbol{T} \begin{bmatrix} L_{ph} & L_m & L_m \\ L_m & L_{ph} & L_m \\ L_m & L_m & L_{ph} \end{bmatrix} \boldsymbol{T}^{-1} \frac{d}{dt} \begin{bmatrix} i_\alpha \\ i_\beta \\ i_0 \end{bmatrix} =$$

$$= \begin{bmatrix} L_{ph} - L_m & 0 & 0 \\ 0 & L_{ph} - L_m & 0 \\ 0 & 0 & L_{ph} + 2L_m \end{bmatrix} \frac{d}{dt} \begin{bmatrix} i_\alpha \\ i_\beta \\ i_0 \end{bmatrix} =$$

$$= \begin{bmatrix} L_\alpha & 0 & 0 \\ 0 & L_\beta & 0 \\ 0 & 0 & L_0 \end{bmatrix} \frac{d}{dt} \begin{bmatrix} i_\alpha \\ i_\beta \\ i_0 \end{bmatrix} \qquad (2)$$

Since $L_\alpha = L_\beta$, the two scalar equations in the α and β variables can be combined in only one equation:

$$\bar{v} = v_\alpha + jv_\beta = L\frac{d}{dt}\left(i_\alpha + ji_\beta\right) = L\frac{d}{dt}\bar{\imath} \qquad (3)$$

where $L = L_\alpha = L_\beta$, and the voltage/current space vectors $\bar{v}$ and $\bar{\imath}$ have been defined as complex-valued time-domain functions. Similar derivations can be readily obtained for resistive and capacitive components.

As far as a three-phase sinusoidal voltage source is considered, by using the Clarke transformation for the source phase voltages $\boldsymbol{e} = [e_a \quad e_b \quad e_c]^T$ we can readily express the corresponding space vector as:

$$\bar{e} = e_\alpha + je_\beta = E_p e^{j\omega t} + E_n^* e^{-j\omega t} \qquad (4)$$

where E_p and E_n are the phasors of the positive and the negative sequence components according to the Symmetrical Component Transformation (SCT) operating in the phasor domain, [23]:

$$\boldsymbol{E}_S = \begin{bmatrix} E_p \\ E_n \\ E_0 \end{bmatrix} = \frac{1}{\sqrt{3}} \begin{bmatrix} 1 & a & a^2 \\ 1 & a^2 & a \\ 1 & 1 & 1 \end{bmatrix} \begin{bmatrix} E_a \\ E_b \\ E_c \end{bmatrix} = \boldsymbol{S}\boldsymbol{E} \qquad (5)$$

where $a = exp(j\,2\pi/3)$, the transformation matrix $\boldsymbol{S}$ is in its rational form such that $\boldsymbol{S}^{-1} = \boldsymbol{S}^{*T}$, and the asterisk denotes complex conjugation.

In the general case, the space vector $\bar{e}$ defined in (4) has an elliptical trajectory on the complex plane characterized by the following semi-major axis r_M, semi-minor axis r_m, and inclination angle φ, [23]:

$$r_M = |E_p| + |E_n^*| \tag{6}$$

$$r_m = \big||E_p| - |E_n^*|\big| \tag{7}$$

$$\varphi = \frac{1}{2}\big[arg(E_p) + arg(E_n^*)\big] \tag{8}$$

In the special case of null negative-sequence component, i.e., $E_n = 0$, the space vector trajectory becomes a circle with radius $|E_p|$.

In order to obtain a complete circuit characterization in the $\alpha\beta 0$ domain, the connections of the three-phase components terminals must be considered. In particular, the star connection (or wye connection) must be investigated as the most common in three-phase power systems. Two kinds of star connections can be recognized. First, a star connection with star center not accessible. Second, a star connection with accessible star center used to interface a single-phase network.

2.1 Star Connection with Non-Accessible Center

This kind of star connection is shown in Figure 2. Voltages are defined with respect to the reference (possibly fictitious) terminal of the whole three-phase system characterized by null total current. Thus, the star connection in Figure 2 can be treated as a three-port network whose independent voltage-current relationships can be written as:

$$v_a = v_b, \quad v_b = v_c, \quad i_a + i_b + i_c = 0 \tag{9}$$

From the Clarke transformation (1), when voltages are considered we readily obtain:

$$v_\alpha = v_\beta = 0 \tag{10}$$

i.e., the star connection with a non-accessible center can be treated as a short circuit in both the α and β domains. Moreover, when currents are considered, from (1) and (9) we readily obtain

$$i_0 = 0 \tag{11}$$

i.e., the star connection with a non-accessible center can be treated as an open circuit in the 0 domain.

2.2 Star Connection with Accessible Center

This kind of star connection is depicted in Figure 3. It is typically used to interconnect a three-phase system (left side) to a single-phase network (right side). In this case the number of ports is four, therefore four independent voltage-current relationships must be written:

$$v_a = v_y, \quad v_b = v_y, \quad v_c = v_y, \quad i_a + i_b + i_c = i_y \tag{12}$$

As far as voltages are considered, from (1) and (12) we readily obtain the same result as (10), i.e., the star connection with an accessible center can be treated as a short circuit in both the α and β domains. Moreover, for the voltage zero component, we obtain:

$$v_0 = \sqrt{3} v_y \tag{13}$$

As far as the currents are considered, from (1) and (12) we obtain:

$$i_0 = \frac{1}{\sqrt{3}} i_y \tag{14}$$

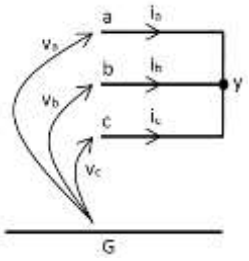

Fig. 2: Star connection with non-accessible center

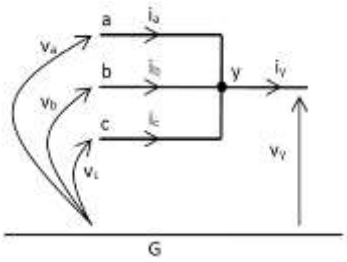

Fig. 3: Star connection with accessible center

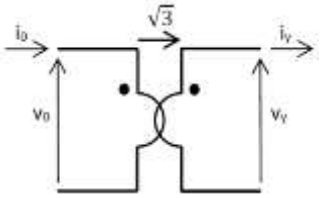

Fig. 4: Zero-component equivalent circuit of a star connection with accessible center

Therefore, from (13) and (14) we obtain that the star connection with accessible center can be represented as an ideal transformer (Figure 4) with turn ratio $\sqrt{3}$ between the zero components of the three-phase system (primary side) and the single-phase network (secondary side). This equivalent representation is useful in applications since all the well-known properties of an ideal transformer can be exploited.

3 Asymmetrical Faults in the Clarke Domain

An asymmetrical fault in a three-phase system can be modeled as a three-phase switch where only one or two switches are operated. A simplified scheme is represented in Figure 5 where a three-phase switch is connected to a generic three-phase system (possibly including single-phase networks).

Since the three-phase switch is operated asymmetrically, however, the general methodology outlined in Section II cannot be used in a straightforward way. A modified methodology can be introduced by resorting to the well-known Thevenin theorem, [24]. Indeed, when the three-phase switch is detached, the remaining circuit is a conventional symmetrical three-phase system that can be treated with the standard technique derived in Section II. Thus, three Thevenin equivalents can be derived in the α,β and 0 domains (Figure 6).

On the other hand, the three-phase switch (Figure 7) can be treated by using the Clarke transformation on the switch variables by setting the constraints of the specific fault under analysis. For example, a faulted phase a (i.e., shorted switch a) can be described by the constraints $v_a = 0, i_b = i_c = 0$. Similarly for the other single-phase or double-phase faults. Such constraints will result in equivalent constraints in the α,β,0 variables, leading to corresponding interconnections of the α,β,0 Thevenin equivalents.

The proposed modified methodology is detailed in the next Subsection for single-phase faults.

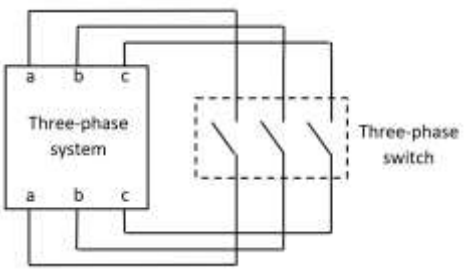

Fig. 5: Three-phase switch connected to a generic three-phase system

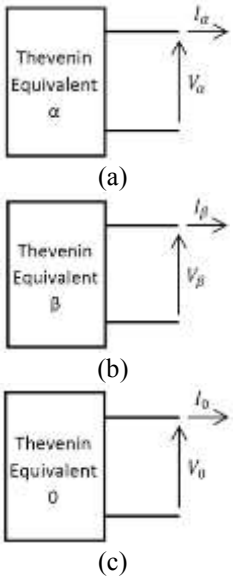

Fig. 6: Thevenin equivalents (α, β, and 0) of the three-phase system connected to the three-phase switch

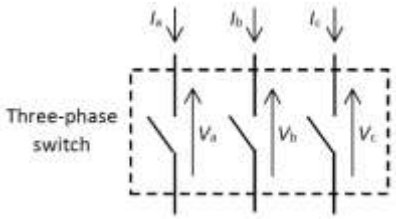

Fig. 7: Three-phase switch and related variables

3.1 Single-phase Faults

A faulted phase a can be modeled by setting the constraints $v_a = 0, i_b = i_c = 0$ in the three-phase switch represented in Figure 7. As far as the voltages are considered, by setting $v_a = 0$ in the Clarke transformation (1) we obtain:

$$\begin{bmatrix} v_\alpha \\ v_\beta \\ v_0 \end{bmatrix} = \sqrt{\frac{2}{3}} \begin{bmatrix} 1 & -\frac{1}{2} & -\frac{1}{2} \\ 0 & \frac{\sqrt{3}}{2} & -\frac{\sqrt{3}}{2} \\ \frac{1}{\sqrt{2}} & \frac{1}{\sqrt{2}} & \frac{1}{\sqrt{2}} \end{bmatrix} \begin{bmatrix} 0 \\ v_b \\ v_c \end{bmatrix} = \sqrt{\frac{2}{3}} \begin{bmatrix} -\frac{1}{2}(v_b + v_c) \\ \frac{\sqrt{3}}{2}(v_b - v_c) \\ \frac{1}{\sqrt{2}}(v_b + v_c) \end{bmatrix} \quad (15)$$

From (15) we obtain the following relationship between Clarke voltages:

$$v_\alpha = -\frac{1}{\sqrt{2}} v_0 \quad (16)$$

As far as the currents are considered, by setting $i_b = i_c = 0$ in the Clarke transformation we obtain:

$$\begin{bmatrix} i_\alpha \\ i_\beta \\ i_0 \end{bmatrix} = \sqrt{\frac{2}{3}} \begin{bmatrix} 1 & -\frac{1}{2} & -\frac{1}{2} \\ 0 & \frac{\sqrt{3}}{2} & -\frac{\sqrt{3}}{2} \\ \frac{1}{\sqrt{2}} & \frac{1}{\sqrt{2}} & \frac{1}{\sqrt{2}} \end{bmatrix} \begin{bmatrix} i_a \\ 0 \\ 0 \end{bmatrix} = \sqrt{\frac{2}{3}} \begin{bmatrix} i_a \\ 0 \\ \frac{1}{\sqrt{2}} i_a \end{bmatrix} \quad (17)$$

From (17) we obtain the following relationships for the Clarke variables:

$$i_\alpha = \sqrt{2} i_0 \quad (18)$$

$$i_\beta = 0 \quad (19)$$

Thus, from (16) and (18) we obtain that the fault constraints can be represented as an ideal transformer with turn ratio $1/\sqrt{2}$ between the α and 0 circuits. Moreover, from (19) we obtain that the β circuit must be set as an open circuit. Thus, the single-phase fault (line *a*) can be represented and analyzed through the equivalent circuits depicted in Figure 8. Similar results can be obtained in the cases where the faulted phase is *b* or *c* instead of *a*. Indeed, a change in the faulted phase results in a $\pm 120^\circ$ shift in the phase of the space vectors.

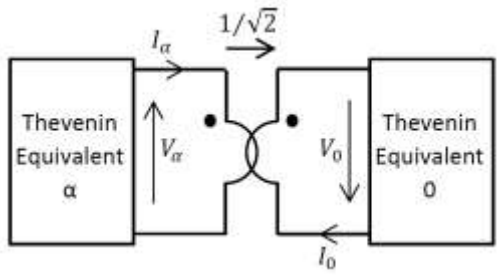

(a)

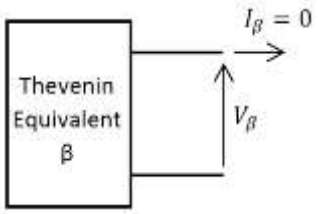

(b)

Fig. 8: Equivalent circuits in the Clarke domain taking into account the single-phase fault on phase *a*

4 Validation for a Radial System

Let us consider the simplified radial system represented in Figure 9. At the Point of Common Coupling (PCC) the source is represented by the equivalent voltage sources E_a, E_b, E_c and the equivalent impedances Z_{eq}. The source is grounded through the impedance Z_g. The line is characterized by the impedance Z_{line}, and the fault location is such that the line left side has impedance xZ_{line} whereas the right side has the impedance $(1-x)Z_{line}$, where $0 < x < 1$. The load is characterized by the impedance Z_L. According to the methodology conventionally used to study grounded faults, however, the load current in the following analysis is neglected, i.e., we assume $Z_L \to \infty$. The grounded fault is characterized by the fault impedance Z_f.

As far as the single-phase fault (phase *a*) to ground is considered, according to the results derived in Section III the equivalent circuits in the Clarke domain are shown in Figure 10. In particular, Figure 10a shows the α and 0 circuits coupled through an ideal transformer with turn ratio $1/\sqrt{2}$. On the other hand, Figure 10b shows the β circuit which is uncoupled to the other circuits and unloaded (i.e., open circuit). The objective of the analysis is the evaluation of the α and β voltages at the PCC. To this aim, the phasor voltages V_α and V_β in Figure 10a and Figure 10b can be readily calculated:

$$V_\alpha = E_\alpha \frac{Z_{eq}/3 + xZ_{line} + Z_f + Z_g}{Z_{eq} + xZ_{line} + Z_f + Z_g} \quad (20)$$

$$V_\beta = E_\beta \quad (21)$$

where $E_\alpha = \sqrt{3}E_a/\sqrt{2}$, $E_\beta = -j\sqrt{3}E_a/\sqrt{2}$, and E_a is the phasor of the phase voltage source *a* in Figure 9. It can be readily shown that (20)-(21) are equivalent to the analytical results derived in [16] through a different methodology based on the circuit solution in the natural *abc* domain.

The sine waves $v_\alpha(t)$ and $v_\beta(t)$ corresponding to the phasors (20)-(21) allow the definition of the voltage space vector

$$\bar{v}(t) = v_\alpha(t) + j v_\beta(t) \quad (22)$$

whose trajectory on the complex plane is an ellipse. According to Figure 1, the inclination of the ellipse in case of faulted phase *a* to ground should be close to 90°.

To assess this point, the following data are assumed to simulate the radial system in Figure 9: $\sqrt{3}E_a = 33$ kV, $Z_{eq} = 1.23 + j18.3\ \Omega$, $Z_{line}/\text{length} = 1.435 + j3.102\ \Omega/\text{km}$, line length = 5 km, $Z_g = Z_f$=0. The location *x* of the faulted phase *a* was treated as a parameter ranging from 0.1 to 1. The corresponding elliptical trajectories of the space vector (22) are represented in Figure 11. Figure 12 shows the same space vectors by assuming 15 km

instead of 5 km for the line length. In both the figures it can be noticed that the ellipse inclination is very close to 90°. In Figure 12, however, the spread of the elliptical shapes is much larger as a consequence of a longer line. Moreover, notice that the changes in Figure 11 and Figure 12 are along the real axes (i.e., the real part of the space vector), whereas along the imaginary axes (i.e., the imaginary part of the space vector) the behavior appears insensitive to the line impedance changes. This is in agreement with (20)-(21) from which it is clear that only the α component is affected by the circuit impedances, whereas the β component is not affected by the circuit impedances because the β circuit is open.

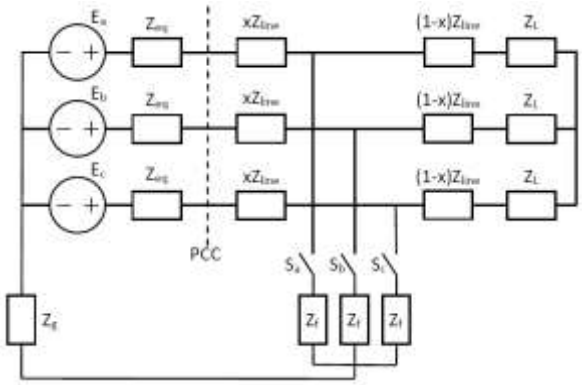

Fig. 9: Radial system used to validate the proposed approach

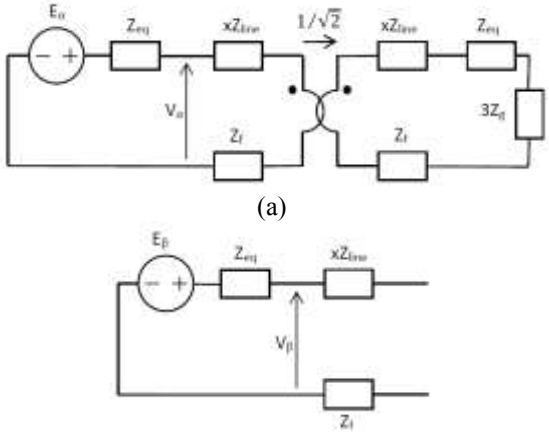

(a)

(b)

Fig. 10: Equivalent circuits in the Clarke domain for the radial system in Figure 9 in case of grounded fault of phase a

Figure 13 shows the effect of ground and fault impedances, i.e., $Z_g = j4\,\Omega$ and $Z_f = 2\,\Omega$ were assumed in the case of line length 5 km. By comparing Figure 13 and Figure 11 a slight change in the ellipse inclination can be noticed as the effect of ground and fault impedances.

Finally, it can be observed that if the faulted phase was b instead of a, the related space vector was simply obtained by rotating by 120° the space vector of the faulted phase a, i.e., $\bar{v}_b = e^{j2\pi/3}\bar{v}$. Similarly, if the faulted phase was c, the related space vector was obtained by rotating by −120° the space vector of the faulted phase a, i.e., $\bar{v}_c = e^{-j2\pi/3}\bar{v}$. As a result, the corresponding ellipse inclinations approach 210° and −30°, respectively, according to Figure 1. The cases of faulted phase b and c are represented in Figure 14 by assuming line length 5 km, $Z_g = j4\,\Omega$ and $Z_f = 2\,\Omega$.

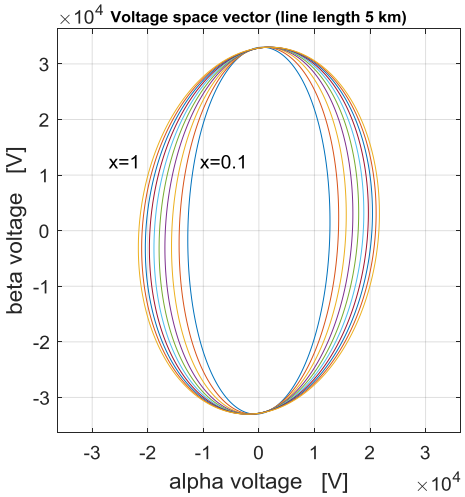

Fig. 11: Trajectory of the voltage space vector for faulted phase a and different locations of the fault. The assumed line length is 5 km. Ground and fault impedances are zero

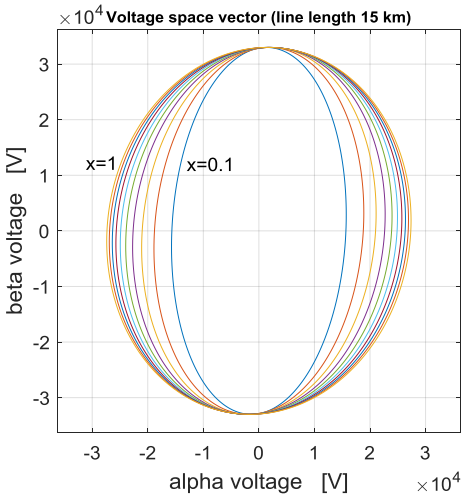

Fig. 12: Trajectory of the voltage space vector for faulted phase a and different locations of the fault. The assumed line length is 15 km

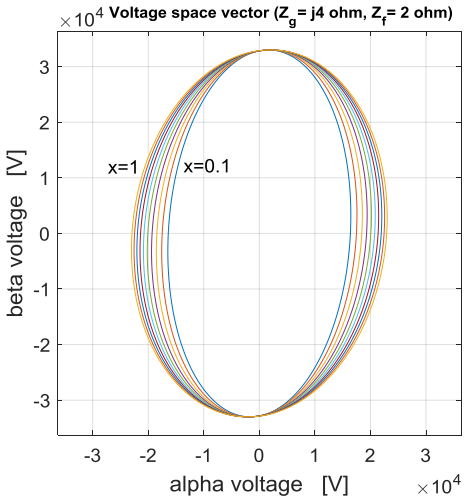

Fig. 13: Trajectory of the voltage space vector for faulted phase *a* and different locations of the fault. The assumed line length is 5 km. Ground and fault impedances are different from zero

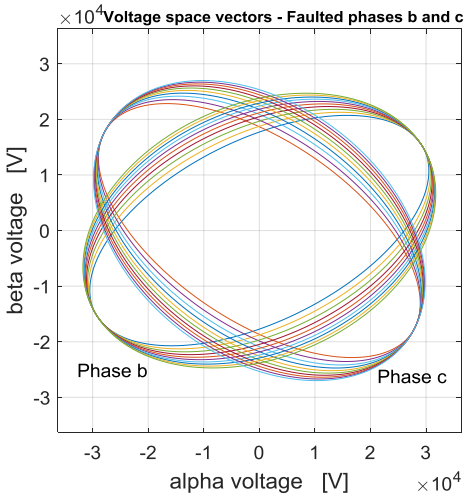

Fig. 14: Trajectory of the voltage space vectors for faulted phases b and c, and different locations of the fault. The assumed line length is 5 km

5 Conclusion

The single-phase to ground fault in a three-phase system has been investigated by introducing equivalent circuits directly in the Clarke domain. Since the derived equivalent circuits allow the direct evaluation of the α and β components of the space vector, the proposed approach allows straightforward interpretation of the properties of the space vector ellipse used to detect and classify the fault.

In particular, the main findings of the paper can be summarized as follows:

- Equivalent circuits have been derived directly in the transformed Clarke variables α, β, 0.
- As a result of the constraints representing the single-phase fault, the α and 0 equivalent circuits are coupled through an ideal transformer. Notice that such a result was obtained thanks to the adopted assumption of Clarke transformation in its power invariant form.
- As far as the β circuit is considered, the fault constraints result in an open circuit. Thus, the β component of the space vector is not involved in the fault.

The proposed methodology has been derived in detail for the case of a single-phase-to-ground fault. Future work will be devoted to extend the results to double-phase faults.

References:

[1] R. C. Dugan, S. Santoso,M. F.McGranaghan, and H.Wayne Beaty, *Electrical Power Systems Quality*, vol. 2. New York, NY, USA: Mcgraw-Hill, 1996.

[2] M. H. Bollen, *Understanding Power Quality Problems: Voltage Sags and Interruptions*. New York, NY, USA: Wiley-IEEE, 2000.

[3] *IEEE Recommended Practice for Monitoring Electric Power Quality*, IEEE Std 1159-2009 (Revision of IEEE Std 1159-1995), Jun. 2009.

[4] P. Wei, Y. Xu, Y. Wu, and C. Li, "Research on the classification of voltage sag sources based on recorded events," *CIRED-Open Access Proc. J.*, vol. 2017, no. 1, pp. 846-850, 2017.

[5] H. Liao, J. V. Milanovic, M. Rodrigues, and A. Shenfield, "Voltage sag estimation in sparsely monitored power systems based on deep learning and system area mapping," *IEEE Trans. Power Del.*, vol. 33, no. 6, pp. 3162-3172, Dec. 2018.

[6] E. Styvaktakis, M. H. J. Bollen, and I. Y. H. Gu, "Expert system for classification and analysis of power system events," *IEEE Trans. Power Del.*, vol. 17, no. 2, pp. 423-428, Apr. 2002.

[7] C. Venkatesh, D. V. S. S. Siva Sarma, and M. Sydulu, "Classification of voltage sag, swell, and harmonics using S-transform based modular neural network," in *Proc. 14th Int. Conf. on Harmonics and Quality of Power*, Bergamo, Italy, 2010, pp. 1-7.

[8] K. M. Silva, B. A. Souza, and N. S. D. Brito, "Fault detection and classification in transmission lines based on wavelet transform and ANN," *IEEE Trans. Power Del.*, vol. 21, no. 4, pp. 2058-2063, Oct. 2006.

[9] P. Janik and T. Lobos, "Automated classification of power-quality disturbances using SVM and RBF networks," *IEEE Trans. Power Del*., vol. 21, no. 3, pp. 1663-1669, Jul. 2006.

[10] M. Manjula, A.V. R. S. Sarma, and S. Mishra, "Detection and classification of voltage sag causes based on empirical mode decomposition," in *Proc. 2011 Annual IEEE India Conf*., Hyderabad, India, 2011, pp. 1-5.

[11] D. Pattanaik, S. Chandra Swain, I. Sekhar Samanta, R. Dash, K. Swain, "Power Quality Disturbance Detection and Monitoring of Solar Integrated Micro-Grid," *WSEAS Transactions on Power Systems*, vol. 17, pp. 306-315, 2022.

[12] Oladapo T. Ibitoye, Moses O. Onibonoje, Joseph O. Dada, "Analysis of Power Quality and Technical Challenges in Grid-Tied Renewable Energy," *WSEAS Transactions on Power Systems*, vol. 18, pp. 248-258, 2023.

[13] V. Ignatova, P. Granjon, and S. Bacha, "Space vector method for voltage dips and swells analysis," *IEEE Trans. on Power Delivery*, vol. 24, no. 4, pp. 2054-2061, 2009.

[14] M. R. Alam, K.M.Muttaqi, and A. Bouzerdoum, "Characterizing voltage sags and swells using three-phase voltage ellipse parameters," *IEEE Trans. Ind. Appl*., vol. 51, no. 4, pp. 2780-2790, Jul. 2015.

[15] J. R. Camarillo-Peñaranda and G. Ramos, "Fault classification and voltage sag parameter computation using voltage ellipses," *IEEE Trans. Ind. Appl.*, vol. 55, no. 1, pp. 92-97, Jan./Feb. 2019.

[16] J. R. Camarillo-Peñaranda and G. Ramos, "Characterization of voltage sags due to faults in radial systems using three-phase voltage ellipse parameters," *IEEE Trans. Ind. Appl*., vol. 54, no. 3, pp. 2032-2040, May/Jun. 2018.

[17] T. García-Sánchez, E. Gómez-Lázaro, E. Muljadi, M. Kessler, A. Molina-García, "Approach to fitting parameters and clustering for characterizing measured voltage dips based on two-dimensional polarisation ellipses," *Renewable Power Generation IET*, vol. 11, no. 10, pp. 1335-1343, 2017.

[18] A. Bagheri, M. J. H. Bollen, "Space phasor model-based monitoring of voltages in three-phase systems", in *Proc. 18th International Conference on Harmonics and Quality of Power (ICHQP) 2018*, 2018, pp. 1-6.

[19] S. Li, L. Xie, and Y. Liu, "Fast Identification Method for Voltage Sag Type and Characteristic," in *Proc. IECON 2019 - 45th Annual Conference of the IEEE Industrial Electronics Society*, Lisbon, Portugal, 2019.

[20] A. Bagheri, M. H. J. Bollen, I. Y. H. Gu, "Improved characterization of multi-stage voltage dips based on the space phasor model", *Electric Power Systems Research*, vol. 154, pp. 319, 2018.

[21] M. R. Alam, K. M. Muttaqi, and A. Bouzerdoum, "A new approach for classification and characterization of voltage dips and swells using 3-D polarization ellipse parameters," *IEEE Trans. Power Del*., vol. 30, no. 3, pp. 1344-1353, Jun. 2015.

[22] M. R. Alam, K. M. Muttaqi and T. K. Saha, "Classification and Localization of Fault-Initiated Voltage Sags Using 3-D Polarization Ellipse Parameters," *IEEE Transactions on Power Delivery*, vol. 35, no. 4, pp. 1812-1822, Aug. 2020.

[23] D. Bellan, "Probability Density Function of Three-Phase Ellipse Parameters for the Characterization of Noisy Voltage Sags," *IEEE Access*, vol. 8, pp. 185503-185513, 2020.

[24] D. Bellan, "Clarke transformation solution of asymmetrical transients in three-phase circuits," *Energies*, vol. 13, pp. 1-19, 2020.

Contribution of Individual Authors to the Creation of a Scientific Article (Ghostwriting Policy)

The authors equally contributed in the present research, at all stages from the formulation of the problem to the final findings and solution.

Sources of Funding for Research Presented in a Scientific Article or Scientific Article Itself

No funding was received for conducting this study.

Conflict of Interest

The authors have no conflicts of interest to declare.